Escape time in anomalous diffusive media

E. K. Lenzi,[1,*] C. Anteneodo,[2,†] and L. Borland[1,‡]
[1]*Centro Brasileiro de Pesquisas Físicas, R. Dr. Xavier Sigaud 150, 22290-180, Rio de Janeiro, Brazil*
[2]*Instituto de Biofísica, Universidade Federal do Rio de Janeiro, Cidade Universitária, CCS, Bloco G, 21941-900, Rio de Janeiro, Brazil*

(Received 1 August 2000; revised manuscript received 23 October 2000; published 23 April 2001)

We investigate the escape behavior of systems governed by the one-dimensional nonlinear diffusion equation $\partial_t\rho=\partial_x[\partial_x U\rho]+D\partial_x^2\rho^\nu$, where the potential of the drift, $U(x)$, presents a double well and D,ν are real parameters. For systems close to the steady state, we obtain an analytical expression of the mean first-passage time, yielding a generalization of Arrhenius law. Analytical predictions are in very good agreement with numerical experiments performed through integration of the associated Ito-Langevin equation. For $\nu\neq 1$, important anomalies are detected in comparison to the standard Brownian case. These results are compared to those obtained numerically for initial conditions far from the steady state.

DOI: 10.1103/PhysRevE.63.051109 PACS number(s): 82.20.Db, 05.40.−a, 05.60.−k, 66.10.Cb

I. INTRODUCTION

The old problem of surmounting a potential barrier, known as Kramers' problem, is doubtlessly relevant in connection with many topics, in fields ranging from physics to finance. It is a key ingredient to understanding phase transitions in complex systems, both in and far from thermal equilibrium. In particular, the quantity known as the escape time (or mean first-passage time) from one stable state to another has found numerous applications in a variety of interesting and novel problems. For example, it plays a key role in stochastic resonance [1] and in describing fluctuation-induced transport such as occurs in kink motion [2] and ratchets [3]. Even the extent of chaos in Hamiltonian systems has been shown to have connections with this quantity [4]. A nice collection of these and other stochastically driven processes can be found in Ref. [5].

However, all of the above examples have been formulated within a standard Brownian framework, for which diffusion properties are normal. In this paper, we look at the problem of calculating the escape time for systems exhibiting anomalous diffusion of the correlated type (in contrast to Levy-type diffusion, which we do not discuss here). An understanding of escape time properties in such systems could open the door for understanding new stochastically driven phenomena. To our knowledge, there has yet been little work done along these lines, although we are aware of some studies relating the anomalous transport properties on a random comb to the distribution of mean first-passage times [6].

The systems we are interested in are such that the diffusion is dependent on the density of particles ρ, resulting in a diffusion coefficient that is proportional to a power $(\nu-1)$ of ρ. Many physical systems are well-described by this class of processes. Let us mention, among other examples, percolation of gases through porous media ($\nu\geqslant 2$) [7], thin saturated regions in porous media ($\nu=2$) [8], gravitational spreading of thin liquid films ($\nu=4$) [9], heat transfer by Marshak waves ($\nu=7$) [10], surface growth ($\nu=3$) [11], spatial diffusion of biological populations ($\nu\geqslant 2$) [12], plasma flows ($\nu<1$) [13], etc. Explicitly, these processes are ruled by an equation of the type known in the literature as the *porous media equation* [14],

$$\partial_t\rho(x,t)=D\partial_x^2[\rho(x,t)]^\nu, \tag{1}$$

where x is a dimensionless coordinate representing a bond length, angle, or any other chemical or physical state variable, t is the dimensionless time, and $\nu D>0$. Rewriting the nonlinear term as $\partial_x(D\nu\rho^{\nu-1}\partial_x\rho)$, it becomes evident that the restriction $D\nu>0$ guarantees that the flux will be from more dense to less dense regions.

Since the nonlinearity in ρ is known to lead to anomalous diffusion if $\nu\neq 1$ [namely superdiffusion for $\nu<1$ and subdiffusion for $\nu>1$ [15,16], as $\langle x^2(t)\rangle\propto t^{2/(\nu+1)}$], important anomalies are also expected when crossing over a barrier is involved. Precisely, we want to unveil here how escape properties are altered when $\nu\neq 1$.

The paper is organized as follows. In Sec. II, we present the systems of interest and discuss some of their general features. Because fluctuations are determined by $\rho(x,t)$ for $\nu\neq 1$, the escape behavior will depend on the initial condition $\rho(x,0)$. Therefore, we first consider systems in the vicinity of the steady state, a condition that allows analytical treatment. Numerical and analytical results for this case are presented in Secs. III and IV, respectively. In Sec. V, we study numerically the escape behavior of systems far from the steady state, comparing the results with the previous ones. Finally, Sec. VI contains concluding remarks.

II. THE SYSTEM

Let us consider a set of identical particles immersed in a thermal environment such as that described by the porous media equation (1). Under the influence of an external bistable potential $U(x)$, introduced in order to probe the escape behavior, the density of particles evolves following the

*Email address: eklenzi@cbpf.br
†Author to whom correspondence should be addressed; email address: celia@cbpf.br
‡Email address: lisa@sphinx.com

nonlinear Fokker-Planck (FP) equation:

$$\partial_t \rho(x,t) = \partial_x [\partial_x U(x) \rho(x,t)] + D \partial_x^2 [\rho(x,t)]^\nu. \qquad (2)$$

This class of equations has been the object of diverse previous studies [15–17].

The stationary solution of Eq. (2) is

$$\rho_s(x) = [1-(\nu-1)\beta V(x)]_+^{1/(\nu-1)}/Z, \qquad (3)$$

where $[f]_+ = \max\{f,0\}$, Z is a (positive) normalization constant, $\beta = Z^{\nu-1}/(\nu D)$, and $V(x) = U(x) - U_o$, with U_o the absolute minimum of the potential. In the limit $\nu \to 1$, the standard linear Fokker-Planck equation is obtained. In such a case, the steady state characterized by the Boltzmann-Gibbs distribution $\rho_s(x) \sim \exp(-U(x)/D)$ is recovered. However, for $\nu \neq 1$, the stationary solutions of Eq. (2) have the form of the maximum Tsallis entropy probability distributions (with Tallis parameter $q = 2-\nu$), as already discussed previously [15–17], even in the absence of external drift [14,18]. It is worth recalling that phemonena such as fully developed turbulence [19], the hadronic transverse moment distribution in high-energy scattering process $e^+e^- \to$ hadrons [20], among others, have been satisfactorily described in terms of distributions similar to Eq. (3) instead of the canonical stationary one.

Steady-state solutions are illustrated in Fig. 1 for a quartic potential. Note that a cutoff condition (Tsallis cutoff), yielding regions with null probability, arises in the $\nu > 1$ case [see Fig. 1(b)]. For a quartic potential, the condition $\nu > -3$ must hold so that the solutions can be normalized. However, the free-particle case requires $\nu > -1$, so we restrict our discussion to this regime.

The nonlinearity in the diffusion term of Eq. (2) accounts for the fact that the environment presents some kind of disorder or long-range correlations in space-time leading to diffusion anomalies. The expression $\beta = Z^{\nu-1}/(\nu D)$ can be interpreted as a generalized Einstein relation for this scenario. Note that in disordered or correlated systems such as those discussed here, the standard Einstein relation is expected to be recovered *in the absence of disorder* [21]. This corresponds to the case of $\nu = 1$ yielding the well-known result $D = 1/\beta$. Also, as was shown in [16], the time-dependent form of these Einstein relations can be used to demonstrate the anomalous scaling properties of these nonlinear diffusion systems. For the free particle one obtains $\langle x^2(t) \rangle \propto 1/\beta(t) \propto Z^2(t) \propto t^{2/(\nu+1)}$.

The Ito-Langevin (IL) counterpart of Eq. (2) reads [15]

$$\dot{x} = -\partial_x U(x) + \sqrt{|D|}\,[\rho(x,t)]^{(\nu-1)/2} \eta(t), \qquad (4)$$

where $\eta(t)$ is a δ-correlated Gaussian noise with zero mean and variance 2. In the particular case $\nu = 1$, the standard Langevin equation for constant noise is recovered. It is noteworthy that this is a phenomenological description, in which the microscopic trajectories are determined by the macroscopic quantity ρ when $\nu \neq 1$. Physically, this represents a kind of statistical feedback. As with state-dependent noise, it is to be seen as the influence of the environment, which is otherwise not explicitly taken into account by the equations of motion. As a particle evolves, it interacts with the environment such that it reacts to the collective density of states around it. We can think of the subdiffusive case as a kind of ''attraction'' to the other particles: Particles tend to stay close to the other particles, fluctuating not far from them. Conversely, we can think of superdiffusive cases as a kind of reaction to the sparseness: If the particle is in a highly populated region, then it is in a sense confined by the other particles, and fluctuations are not so large, but as soon as it gets into less dense regions it does not experience this confinement and fluctuations can get very large.

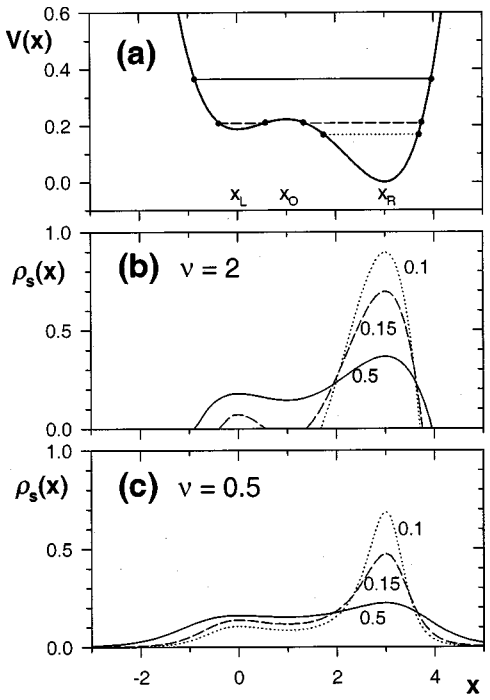

FIG. 1. The cutoff condition. (a) Dimensionless double-well potential $V(x) = ax^4 + bx^3 + cx^2 + d$, with $a = \frac{1}{48}, b = -\frac{1}{9}, c = \frac{1}{8}, d = \frac{3}{16}$. The stationary distribution $\rho_s(x)$ is shown for $\nu = 2$ (b) and 0.5 (c), for different values of D as indicated in the figure. For $\nu \leqslant 1$, the full state space is covered with power-law tails. For $\nu > 1$, a cutoff restricts the attainable space. Observe in (b) that as D decreases, particles become more confined until only the neighborhood of the deepest valley is allowed. The horizontal lines in (a) represent the cutoff condition $V(x) = 1/\beta$, which defines the allowed regions for $\nu = 2$ and the same values of D as in (b). All quantities are dimensionless.

III. NUMERICAL RESULTS IN THE VICINITY OF THE STEADY STATE

For numerical experiments we chose as a prototype of the double-well potential the quartic polynomial $V(x) = ax^4 + bx^3 + cx^2 + d$. The coefficients were chosen as in Fig. 1, for which $(x_L, x_O, x_R) = (0,1,3)$, with x_L, x_O, and x_R corresponding to the bottom of the left-hand well, the top of the barrier, and the bottom of the right-hand well, respectively. We studied the escape behavior close to the steady state. That is, once a population of a large number of particles has already attained the steady state described by Eq. (3), a probe was injected at x_L. Then its trajectory was obtained by solv-

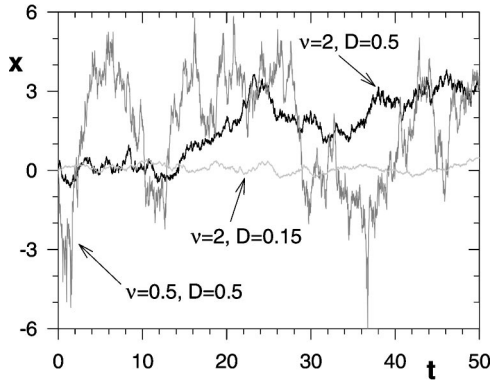

FIG. 2. Typical trajectories x vs t for $(\nu,D)=(0.5,0.5)$ (dark gray), (2,0.5) (black), and (2,0.15) (light gray).

ing, following the numerical scheme in Ref. [22], the IL (4) for $\rho(x,t)=\rho_s(x)$, starting from $x(t=0)=x_L$. Typical trajectories are displayed in Fig. 2. For $\nu>1$, fluctuations are reduced and trajectories result confined to the region within the cutoff boundaries [see also Fig. 1(b)]; moreover, when the diffusion constant D is smaller than a critical value D_c (here $D_c\simeq 0.17$ for $\nu=2$), the state space becomes disconnected and crossings become forbidden. For $\nu<1$, the amplitude of noise is enhanced in the regions of low density and the entire space tends to be populated.

We measured the mean first-passage time, i.e., the average time interval $T(x_L\rightarrow x)$ that a particle at x_L takes to reach for the first time a given state $x>x_L$. In Fig. 3, we present plots of $T(x)\equiv T(x_L\rightarrow x)$ vs x. For $\nu\geqslant 1$ [Fig. 3(a)], plateaus become evident as D approaches D_c, indicating that most of the time is spent overcoming the barrier around x_O. On the other hand, for $\nu<1$ [Fig. 3(b)], the passage time is sensitive to the exact final state and there is not a well-defined plateau, even in the small-D regime. Moreover, as D decreases, the curves collapse to a limiting one for states below x_R, but grow faster above x_R, diverging in the limit $D\rightarrow 0$. The escape behavior seems to be discontinuous at

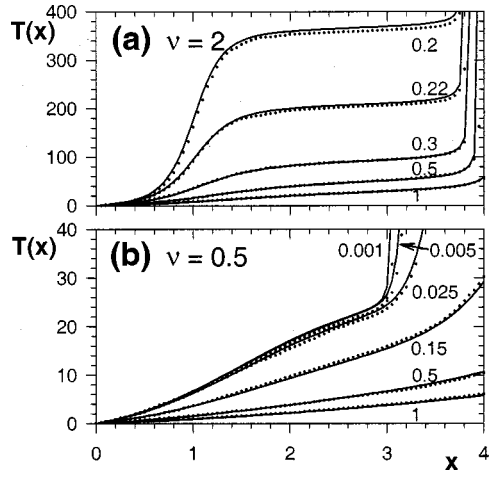

FIG. 3. $T(x)\equiv T(x_L\rightarrow x)$ vs x for different values of D indicated in the figure and $\nu=2$ (a) and 0.5 (b). Circles correspond to numerical experiments (mean value over 1000 realizations) and full lines to theoretical prediction given by Eq. (6).

$D=0$. In fact, for $D=0$ there is no diffusion, however for finite D the particle is attracted towards the deepest valley at x_R and becomes trapped within a typical time interval that is bounded from above. This effect can be understood keeping in mind that fluctuations depend on D not only through the factor $\sqrt{|D|}$ but also by means of the density through a factor that, for $\nu<1$, becomes very large outside the neighborhood of the absolute minimum where particles tend to concentrate as $D\rightarrow 0$. In other words, the deterministic case is not recovered when $D\rightarrow 0$ since the effective diffusion coefficient $D\rho^{\nu-1}$ does not vanish in that limit due to the singularity at $\rho=0$.

IV. ANALYTICAL CONSIDERATIONS

Let us show that these results can be understood analytically. For a system in the vicinity of the steady state, we can consider the following approximation for Eq. (2):

$$\partial_t\rho(x,t)\simeq\partial_x[\partial_x U(x)\rho(x,t)]+D\partial_x^2[\{\rho_s(x)\}^{\nu-1}\rho(x,t)]. \tag{5}$$

Once the FP equation is linear, the problem of escape from a well can be treated directly, following the same lines as for homogeneous processes characterized by time-independent drift and diffusion coefficients [23]. Basically, an equation for the probability that the particle is still within a given interval of state space at time t is found using the corresponding backward Fokker-Planck equation and solved under appropriate boundary conditions. In this way, one finds that the mean first-passage time $T(x_1\rightarrow x_2)$, for $x_1<x_2$, is given by

$$T(x_1\rightarrow x_2)=|\nu|\beta\int_{x_1}^{x_2}[1-(\nu-1)\beta V(y)]_+^{|\nu|/(1-\nu)}dy \times\int_{-\infty}^{y}[1-(\nu-1)\beta V(z)]_+^{\mu/(\nu-1)}dz, \tag{6}$$

where $\mu=1$ if $\nu>0$ and $\mu=1-2\nu$ if $\nu<0$. Expression (6) reproduces numerical experiments with excellent agreement, as illustrated in Fig. 3.

In Fig. 4, we show $T\equiv T(x_R)\equiv T(x_L\rightarrow x_R)$ as a function of $1/D$ (full lines), for different values of $\nu>0$, as calculated from Eq. (6). T represents a measure of the escape time from the left- to the right-hand well, even in the $\nu<1$ cases where plateaus are not well defined. In the range $\nu>1$, T diverges at a value D_c, defined by the cutoff prescription, below which the right-hand well becomes inaccessible. In the $0<\nu<1$ case, T saturates as $1/D$ increases. The hyperdiffusive regime $\nu<0$ (hence $D<0$), where spreading is faster than ballistic, demonstrates the same general features discussed for the region $0<\nu<1$, but $|D|$ must be considered instead of D. For any ν and small $1/|D|$, the escape time follows the power law $T\sim\beta^{3/4}\sim 1/|D|^{3/(\nu+3)}$.

If $x_1\simeq x_L$ and $x_2\simeq x_R$, then it is possible to find an approximate expression for the escape time T when $|D|$ (hence $1/\beta$) is sufficiently small, noting that the integrands in Eq. (6) present sharp peaks at x_O and x_L, respectively. In that

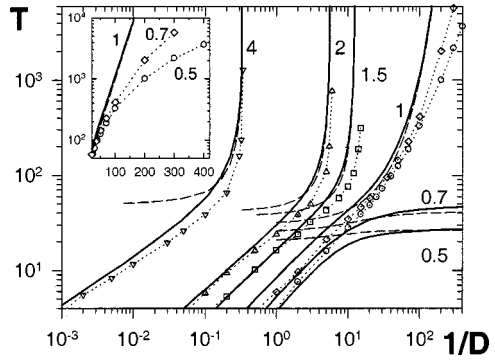

FIG. 4. Escape time $T \equiv T(x_R)$ as a function of $1/D$, for different values of $\nu > 0$ indicated in the figure. Full lines are generated from Eq. (6). Dashed lines correspond to the low-D approximation given by Eq. (7). Symbols correspond to the initial condition where all the particles (at least 1000) are injected at the same time at x_L. Dotted lines are guides for symbols. Inset: Detail (semilog) of the low-D region for $\nu \leqslant 1$.

case, the integrals can be evaluated by a saddle-point approximation extending the integration limits to the whole space. Following this procedure, we arrive at

$$T \simeq \frac{2\pi}{\sqrt{\omega_L \omega_O}} \frac{2|\nu|}{|\nu|+\mu} \left(\frac{1-(\nu-1)\beta V(x_O)}{1-(\nu-1)\beta V(x_L)} \right)^{(|\nu|+\mu)/[2(1-\nu)]}, \tag{7}$$

where ω_L and ω_O are the frequencies at the bottom of the left well and at the top of the barrier, respectively. Expression (7) is a generalization of the Arrhenius law, which, as expected, is recovered in the limit $\nu \to 1$. In fact, in that limit, $T \simeq (2\pi/\sqrt{\omega_L \omega_O}) \exp(\Delta V/D)$, where $\Delta V \equiv V(x_O) - V(x_L)$ is the barrier height.

For comparison, the approximation given by Eq. (7) is also exhibited in Fig. 4 (dashed lines). The approximation is good for large $1/|D|$, as expected. It works better for $\nu > 1$. Let us comment on the main features revealed by this expression. When $\nu > 1$, it foresees the divergence of T at finite D. In fact, D_c is obtained from $1/\beta_c \simeq (\nu-1)V(x_O)$. When $\nu < 1$, saturation of T for large $1/|D|$ is also predicted [unless $V(x_L) = 0$] since β is an unbounded increasing function of $1/|D|$. If $V(x_L) = 0$, then Eq. (7) indicates that T diverges for vanishing $|D|$. In particular, if $0 < \nu < 1$, $T \sim \beta^{(\nu+1)/[2(1-\nu)]} \sim 1/D^{1/(1-\nu)}$ and the deterministic limit is achieved. In the limit $\nu \to 1$, the exponential growth of T with $1/D$ is always recovered.

V. NUMERICAL RESULTS FAR FROM THE STEADY STATE

The problem in the vicinity of the steady state actually corresponds to a linear one with a state-dependent diffusion coefficient. However, it allows an analytical treatment that can be kept in mind as a reference when studying more general cases. In order to test how the previous results compare to those of a more general situation, we also performed numerical studies of the escape properties far from the steady state. Particularly, we studied the case in which particles are injected all at the same time at x_L. This instance requires simultaneous integration of the FP equation, in order to follow the evolution of $\rho(x,t)$ starting from $\rho(x,0) = \delta(x - x_L)$, together with integration of the IL equation (4), starting from $x(t=0) = x_L = 0$. Now, the parameter ν must lie in the region $\nu > 0$ due to the divergence in Eq. (2). An implicit finite-difference scheme with centered space differences was employed for numerical integration of the nonlinear FP equation [24]. The time evolution of the density is illustrated in Fig. 5.

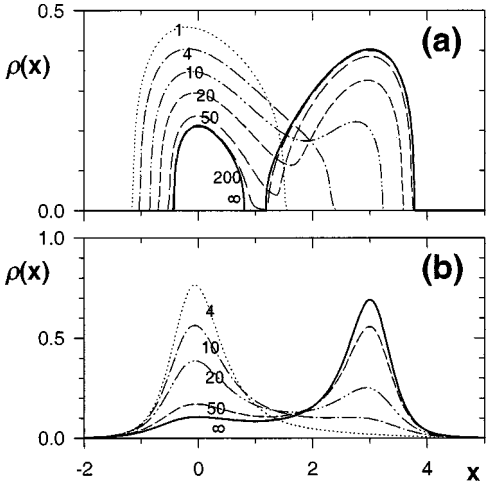

FIG. 5. Time evolution of the density of particles obtained by numerical integration of Eq. (2) with $\rho(x,0) = \delta(x)$ for $(\nu, D) = (4.0, 2.5)$ (a) and (0.5,0.1) (b). The profiles correspond to times t indicated in the figure.

The escape time T as a function of $1/D$ (symbols) obtained for different values of ν was included in Fig. 4. Let us compare this case to the precedent steady one. For sufficiently large D, T is not sensitively dependent on the initial distribution and Eq. (6) fits well to the numerical results for any $\nu > 0$, following the power law $T \sim 1/D^{3/(\nu+3)}$ derived above. On the other hand, for small D, crossing times become closer to those of the standard case $\nu = 1$ for any ν. This can be understood as follows. For $\nu > 1$, passage times are smaller than those given by Eq. (6) since, as the distribution evolves, there is an initial passage even between regions disconnected at the steady state [see Fig. 5(a)]. However, our results suggest that the divergence of T for a finite critical D, close to D_c, still occurs. On the other hand, in the range $\nu < 1$, crossing times are larger than those given by Eq. (6) since now the density of particles is initially unfavorable for surmounting the barrier [see Fig. 5(b)]. Saturation is not observed and the escape time increases with $1/D$ apparently following a power law. It is worth noting that, as derived above, a power law with exponent $1/(1-\nu)$ is the one expected if the average effective potential felt by crossing particles has the absolute minimum at x_L, which is consistent with the observed density evolution [see Fig. 5(b)].

VI. FINAL REMARKS

Summarizing, we have obtained the escape time for systems exhibiting anomalous diffusion due to a stochastic non-

linear dependency on the density. For steady-state conditions, we obtain an analytical expression for the mean first-passage time whose predictions are in excellent agreement with numerical results (Fig. 3). This analytical expression yields a generalization of Arrhenius law. A behavior quite different from that of the standard Brownian case $\nu=1$ is depicted. Under close to stationary conditions, two regimes are detected: In the region $\nu<1$ (superdiffusion), the escape time T saturates for vanishing D, if $V(x_L)\neq 0$, and grows with $1/D$ following a power law otherwise. In the region $\nu>1$ (subdiffusion), T diverges at D_c (Fig. 4).

These results give hints of what should be expected in more general cases. For systems far from the steady state, T grows with $1/D$ apparently following a power law in the superdiffusive cases while T diverges at finite D in the subdiffusive ones.

ACKNOWLEDGMENTS

We want to thank R. O. Vallejos for enlightening discussions. We acknowledge Brazilian Agencies, CNPq, and FAPERJ for partial financial support.

[1] B. McNamara, K. Wiesenfeld, and R. Roy, Phys. Rev. Lett. **60**, 2626 (1988).
[2] M. Büttiker, Z. Phys. B: Condens. Matter **68**, 161 (1987); N.G. van Kampen, IBM J. Res. Dev. **32**, 107 (1988); R. Landauer, J. Stat. Phys. **53**, 233 (1988).
[3] M. Magnasco, Phys. Rev. Lett. **71**, 1477 (1993).
[4] P. Alpatov and L.E. Reichl, Phys. Rev. E **52**, 4516 (1995).
[5] *Fluctuations and Order: The New Synthesis*, edited by M. Millonas (Springer, New York, 1996).
[6] S. Revathi, V. Balakrishnan, S. Lakshmibala, and K.P.N. Murthy, Phys. Rev. E **54**, 2298 (1996).
[7] M. Muskat, *The Flow of Homogeneous Fluids through Porous Media* (McGraw-Hill, New York, 1937).
[8] P. Y. Ploubarinova-Kochina, *Theory of Ground Water Movement* (Princeton University Press, Princeton, NJ, 1962).
[9] J. Buckmaster, J. Fluid Mech. **81**, 735 (1977).
[10] E.W. Larsen and G.C. Pomraning, SIAM (Soc. Ind. Appl. Math.) J. Appl. Math. **39**, 201 (1980).
[11] H. Spohn, J. Phys. I **3**, 69 (1993).
[12] M.E. Gurtin and R.C. MacCamy, Math. Biosci. **33**, 35 (1977).
[13] P. Rosenau, Phys. Rev. Lett. **74**, 1056 (1995); A. Compte, D. Jou, and Y. Katayama, J. Phys. A **30**, 1023 (1997).
[14] L. A. Peletier, in *Application of Nonlinear Analysis in the Physical Sciences*, edited by H. Ammam and N. Bazley (Pitman, Boston, 1981), p. 229.
[15] L. Borland, Phys. Rev. E **57**, 6634 (1998).
[16] C. Tsallis and D.J. Bukman, Phys. Rev. E **54**, R2197 (1996); A.R. Plastino and A. Plastino, Physica A **222**, 347 (1995).
[17] A. Rigo, A.R. Plastino, M. Casas, and A. Plastino, Phys. Lett. A **276**, 97 (2000); D.A. Stariolo, *ibid.* **185**, 262 (1994).
[18] A. Compte, D. Jou, and Y. Katayama, J. Phys. A **29**, 4321 (1996).
[19] T. Arimitsu and N. Arimitsu, Phys. Rev. E **61**, 3237 (2000); J. Phys. A **33**, L235 (2000); C. Beck, Physica A **277**, 115 (2000); C. Beck, G. S. Lewis, and H. L. Swinney, Phys. Rev. E **63**, 035303(R) (2001).
[20] I. Bediaga, E.M. Curado, and J. Miranda, Physica A **286**, 164 (2000).
[21] J.P. Bouchaud and A. Georges, Phys. Rep. **195**, 127 (1990).
[22] H. Risken, *The Fokker-Planck Equation*, 2nd ed. (Springer, Berlin, 1984).
[23] C. W. Gardiner, *Handbook of Stochastic Methods*, 2nd ed. (Springer, Berlin, 1994).
[24] R. D. Richtmyer, *Difference Methods for Initial-value Problems*, 1st ed. (Interscience Publishers, New York, 1957).